

Exon sequences distant from the splice junction are required for efficient self-splicing of the *Tetrahymena* IVS

Sarah A. Woodson

Department of Chemistry and Biochemistry, University of Maryland at College Park, College Park, MD 20742-2021, USA

Received April 10, 1992; Revised and Accepted June 30, 1992

ABSTRACT

The presence of a natural rRNA secondary structure element immediately preceding the 5' splice site of the *Tetrahymena* IVS can inhibit self-splicing by competing with base pairing between the 5' exon and the guide sequence of the IVS (P1). Formation of this alternative hairpin is preferred in short precursor RNAs, and results in loss of G-addition to the 5' splice site. Pre-rRNAs which contain longer exons of ribosomal sequence, however, splice rapidly. As many as 146 nucleotides of the 5' exon and 86 nucleotides of the 3' exon are required for efficient self-splicing of *Tetrahymena* precursors. The presence of nucleotides distant from the 5' splice site apparently alters the equilibrium between the alternative hairpins, and promotes formation of active precursors. This effect is dependent on the specific sequences of the ribosomal pre-RNA, since point mutations within this region reduce the rate of splicing as much as 50-fold. This system provides an opportunity to study the way in which long-range interactions can influence splice site selection in a highly structured RNA.

INTRODUCTION

The mechanism of splice site recognition is a central problem in RNA processing, and has recently been the focus of much research. In splicing of group I and group II introns, base pairing between the 5' exon and a sequence (or sequences) within the intron is required for 5' splice site recognition. In nuclear pre-mRNAs, consensus sequences for 5' and 3' splice sites have been identified (reviewed in ref 1). In part, recognition of the 5' splice site is achieved by binding of the U1 snRNP, presumably through base pairing between the U1 snRNA and the conserved nucleotides at the 5' splice site (2).

In addition to these simple base pairing motifs, however, both binding of proteins to the RNA, and higher order structure within the pre-RNA itself may enhance or repress the use of potential splice sites. For example, the protein factor(s) ASF and SF2 have been shown to alter 5' splice site use in SV40 and human β -globin pre-mRNAs (3,4). In addition to binding of protein factors, the structure of the precursor RNA and the nature of the exon sequences can strongly influence recognition and activation of

potential splice sites (5–7). Tissue-specific splicing of the β -tropomyosin pre-mRNA depends on the formation or disruption of a stable secondary structure (8,9).

Exon secondary structure adjacent to the 5' splice site has been shown to affect splicing of the *Tetrahymena* IVS (intervening sequence, or intron) (10). In this relatively simple system, self-splicing can be observed *in vitro* in the absence of protein co-factors. Thus any change in the reactivity of the precursor can be attributed to interactions within that particular RNA. Experiments presented here show that additional exon sequences removed from the 5' splice site promote efficient processing of *Tetrahymena* precursors.

Self-splicing of the *Tetrahymena* IVS has been described in detail (reviewed in ref. 11), and requires only magnesium ion and a guanosine or GTP co-factor, in addition to the properly folded IVS RNA. Recognition of the 5' splice site is achieved by Watson–Crick base pairing between nucleotides preceding the 5' splice site and the internal guide sequence (IGS) of the IVS (12,13). This pairing, termed P1, is conserved among group I introns, and is required for both forward and reverse self-splicing.

The natural splice junction of the *Tetrahymena* IVS is immediately preceded by another stable hairpin that is highly conserved among large subunit rRNAs. The stem of this hairpin involves the same nucleotides of the 5' exon that normally participate in P1. Consequently, a precursor containing natural exon sequences can adopt two alternative pairings, as diagrammed in Figure 1a. It can either form the hairpin within the 5' exon, designated P(-1) (10), or it can form the pairing between the 5' exon and the internal guide. As outlined in Figure 1b, precursors containing P(-1) do not permit the 5' splice site to be activated in the normal fashion, and are not expected to form spliced products.

Previous work has shown that in short transcripts that contain only a 20 nucleotide 5' exon and a 29 nucleotide 3' exon, the ability to form a stable P(-1) pairing does in fact inhibit splicing (10). Surprisingly, the presence of the wild-type P(-1) lowered the rate of splicing in these short precursors 20-fold, although the estimated stabilities of P(-1) and P1 are comparable (14). The lower reactivity of this short precursor (TZIVS Δ 12) is due to loss of P1 and 5' splice site activation, since it does undergo an intermolecular splicing reaction with an exogenous 5' exon.

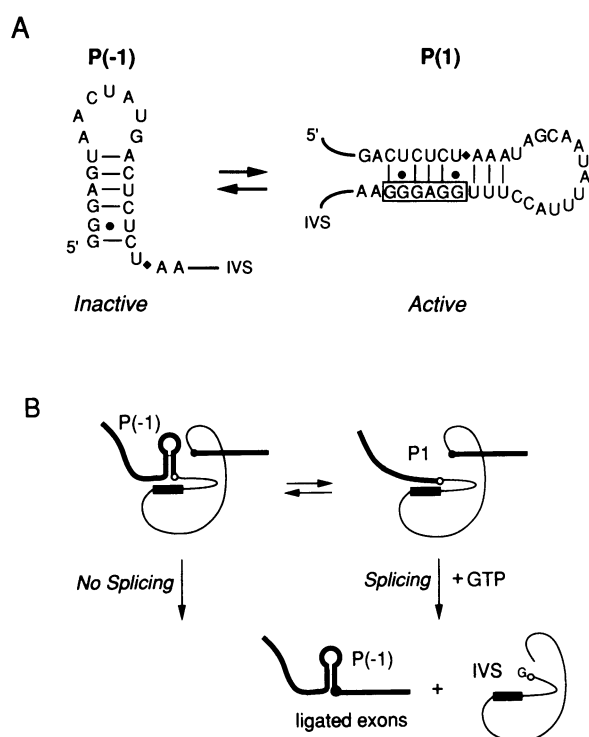


Figure 1. Alternative hairpins in RNA precursors. **A.** Sequence of alternative hairpins P(-1) and P1. P(-1) is conserved in the large subunit rRNAs, P1 is conserved among group I introns, and is required for self-splicing. The internal guide sequence (IGS) is boxed in the right panel. The 5' splice site is indicated by ♦. **B.** Equilibrium between inactive and active conformers of precursors. Conformers containing P(-1), shown on the left, are blocked in the first step of splicing. Precursors containing P1 can go on to form the normal spliced products, which are the ligated exons and linear IVS RNAs. Following excision of the intron, the ligated exons can refold to form P(-1). Shaded box, IGS; open circle, 5' splice site; thick line, exon sequences; thin line, IVS.

These results initially appeared to contradict earlier work on full-length pre-rRNA made in isolated *Tetrahymena* nuclei, which splices efficiently under similar conditions (15). I have further investigated splicing of transcripts that contain longer exons from the *Tetrahymena* ribosomal rRNA. The data presented here show that additional exon sequences can relieve inhibition due to P(-1) and permit efficient self-splicing of the pre-rRNA *in vitro*. This in turn implies that long-range interactions within the exon can influence the equilibrium between the alternative P(-1) and P1 hairpins at the 5' splice site.

MATERIALS AND METHODS

Materials

DNA oligonucleotides were synthesized by the phosphoramidite method. Nucleoside triphosphates were purchased from Pharmacia, and radiolabeled nucleotides from New England Nuclear. Restriction enzymes, DNA polymerase Klenow fragment, mung bean nuclease, and Eco RI linkers (# 1019) were purchased from New England Biolabs. T_4 polynucleotide kinase, T_4 DNA ligase, T_4 DNA polymerase and S1 nuclease were obtained from US Biochemicals. Exonuclease III was from Promega. T_7 RNA polymerase was purified by the procedure of Studier and coworkers (16). Plasmids pTZ19U and pTZ18U were from Bio-Rad.

Plasmid construction and mutagenesis

Plasmids pTT1A3 (17) and pTZIVS Δ 12 (10) have been described previously. Plasmid JK43-T₇ was constructed from pJK43-SP6 (18), and was a generous gift of A. Zaugg.

pJK43i29 and *pTZ Δ 12i624*. In order to exchange the 3' exon fragments of pTZIVS Δ 12 and pJK43-T₇, the Hind III site of pTZIVS Δ 12 was first converted to an Eco RI restriction site in pTZIVS Δ 12E. pTZIVS Δ 12 DNA was digested with Hind III and the ends filled in with Klenow DNA polymerase. Eco RI linkers were blunt-end ligated to the linear plasmid DNA, digested with Eco RI, and the plasmid DNA recircularized with DNA ligase. pJK43i29 and pTZ Δ 12i624 were constructed by exchanging the 629 and 34 base pair Sca I-Eco RI fragments of pJK43-T₇ and pTZIVS Δ 12E, respectively, with each other.

Mutagenesis. Oligonucleotide-directed mutagenesis was carried out by the method of Kunkel (19). The 1.3 kb Hind III-Eco RI fragment of JK43-T₇ was subcloned into the polylinker of pTZ18U (pJK43-TZ18). Single-stranded deoxyuridine-containing DNA was then isolated from *E. coli* strain CJ236. Plasmid DNA containing the desired changes was identified by dideoxy sequencing, and the mutated HindIII-Eco RI fragments were reisolated and subcloned into pTZ19U for *in vitro* transcription. Plasmids listed in Table II were obtained by mutagenesis of pJK43-TZ18.

Exon deletions. Using the strategy outlined above, 3' exon deletion mutants were constructed by introducing a Sma I site either 421, 229 or 70 base pairs downstream from the 3' splice site and a Pst I site 48 bp downstream from the 3' splice site. These sites correspond to *Xenopus* 28 S rRNA positions 3356, 3164, 3005, and 2983. 5' exon deletion mutants were similarly obtained by introducing a new Hind III site 120 or 55 bp upstream from the 5' splice site (*Xenopus* positions 2814 and 2881). The new Hind III-Eco RI fragment was subcloned into pTZ19U, as above. Plasmid SW010 was made by simultaneously introducing a Hind III site 120 bp upstream and a Sma I site 70 bp downstream of the IVS.

Plasmid SW012 was constructed by linearizing pJK3164 DNA with Sma I, digestion with Exo III and S1 nuclease followed by mung bean nuclease, and blunt-end ligation of Eco RI linkers. pJK3021 was selected from the transformants as having the highest self-splicing activity in the pre-rRNA. A new Hind III site in the 5' exon of pJK3021 was created in the same manner, and the resulting 641 bp Hind III-Eco RI fragment was recloned into pTZ19U to give pSW012.

Preparation of precursor RNA

Precursor RNA was transcribed from linear plasmid DNA using T_7 RNA polymerase as described previously (10). Plasmids pJK3005, pJK3164, pJK3364 and pSW010 were restricted with Sma I, pJK2983 with Pst I, and pTZIVS Δ 12 with Hind III. All others were linearized with Eco RI. RNA transcripts were uniformly labeled by the incorporation of [α - 32 P]ATP. Precursor RNA was isolated from 8 M urea polyacrylamide gels as described.

Self-splicing reactions

Splicing of precursor RNAs was carried out in 100 mM $(\text{NH}_4)_2\text{SO}_4$, 50 mM HEPES, pH 7.5, 5 mM MgCl_2 , 100 μM GTP at 30°C, as described previously (Woodson and Cech, 1991). Prior to beginning the reaction, the RNA was heated to

95°C for 1 min and cooled rapidly in the presence of splicing buffer minus GTP (20). The mixture was incubated 1 min at 30°C, and the splicing reaction initiated with the addition of GTP. Aliquots were removed at specified times and added to an equal volume of gel loading buffer containing 10 M urea. Samples were electrophoresed on 8M urea, 4% polyacrylamide gels. Radioactivity in each lane was quantitated using either an AMBIS radioanalytic scanner or a Molecular Dynamics PhosphorImager.

The fraction of ligated exon RNA, $f(\text{LE})$, was determined for each lane by dividing the radioactivity in the ligated exon band by the total radioactivity of all reaction products. The fraction of spliced products, $f(\text{sp})$, is equal to $f(\text{LE})$ divided by the fraction of radioactivity calculated to be in the exon portion of the precursor (0.682 for JK43). The observed rates of splicing (k_{obs}) were determined from linear fits to $\ln[1-f(\text{sp})]$ vs. time (minutes) at initial times, normalized to the fraction of precursor reacted after 4–6 hours of incubation. Typically, 55–65% of the precursor RNAs splice during the initial linear portion of the curve, and better than 85% have reacted by the end of the assay. In the case of a few very unreactive precursors, such as TZIVS Δ 12 and JK3'mis, only 40% of the pre-RNA splices linearly. Despite care taken in preparation of RNA samples, rates typically vary 10–20% between preparations. Reported activities reflect several (2–5) isolations and rate determinations for a given precursor. We have recently obtained similar results using RNA transcripts isolated directly from *in vitro* transcription reactions.

3' Splice Site Hydrolysis.

Precursor RNA was incubated in 50 mM CHES, pH 9.0, 200 mM NaCl, 10 mM MgCl₂ at 42°C in the absence of GTP, for up to 60 min. Rates were determined from linear fits to $\ln[f(\text{pre})]$ vs. time for the first 15 minutes of the time course, where $f(\text{pre})$ is the fraction of radioactivity remaining in the precursor band for each lane.

RESULTS

Self-splicing of long and short precursor RNAs

In order to examine the effect of additional ribosomal exon sequences, the rates of self-splicing of *Tetrahymena* precursor RNAs of differing lengths were compared under standard conditions, as shown in Figure 2. As seen previously, the short precursor, TZIVS Δ 12, does not self-splice efficiently, due to preferential formation of P(-1) over P1 (10). In contrast, precursor JK43, which contains much longer exons, does splice rapidly under these conditions, even though it can still potentially form P(-1). Precursor TT1A3 splices at an intermediate rate.

Splicing rates were determined for each precursor, and are listed in Table I and shown in Figure 3. Precursor JK43 splices at a rate of 0.50 min⁻¹, much faster than TZIVS Δ 12, and similar to the rate measured for *in vivo* isolated pre-rRNA (15). The greater reactivity of JK43 implies that P1 is formed more readily than in TZIVS Δ 12. Thus the longer transcript must provide a mechanism for ensuring efficient excision of the IVS, despite the possibility of forming an inhibitory hairpin within the 5' exon.

Although the short TZIVS Δ 12 precursor does not splice readily, it can undergo hydrolysis at the 3' splice site (10). This hydrolysis reaction occurs in the absence of GTP, is stimulated by high pH, and depends on the folded form of the IVS RNA (21, 22). The ability to observe specific 3' splice site hydrolysis is another measure of the catalytic potential of the IVS,

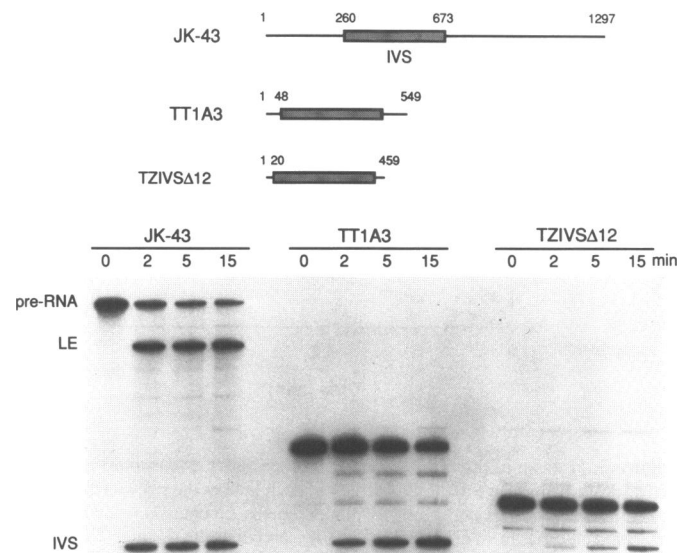


Figure 2. Self-splicing of precursors containing long and short exon sequences. The lengths of the exon sequences are diagrammed at the top of the figure for each precursor. Precursor JK43 contains 260 nucleotides (nt.) of ribosomal sequence upstream of the 5' splice site and 624 nt. of the 3' exon in addition to the IVS. The 5' exon of pTT1A3 contains 33 nt. of natural sequence plus 15 nt. of vector sequence. The first 38 nt. of the 3' exons are from ribosomal sequences, followed by 50 bases of vector sequence. Plasmid TZIVS Δ 12 encodes the very short precursor described previously (13), containing only the 20 base pairs comprising P(-1) in the 5' exon, and a 29 base pair 3' exon. Splicing reactions were carried out at 30°C in the presence of 100 μ M GTP as described. The reactions were stopped at the time (minutes) shown above each lane, and the RNA electrophoresed on an 8 M urea, 4% polyacrylamide gel. Pre-RNA indicates the JK43 precursor, LE denotes the ligated exon product of precursor JK43, IVS marks the position of the linear IVS RNA. Lighter product bands above the IVS for TZIVS Δ 12 result from hydrolysis at the 3' splice site. Minor products of TT1A3 are the 5'exon-IVS hydrolysis product, and the IVS-3'exon intermediate. The 136 nt. and 49 nt. ligated exon products of TT1A3 and TZIVS Δ 12, respectively, have migrated off the gel.

Table I. Splicing and 3' splice site hydrolysis of precursors with exons of differing length.

Precursor	5' exon ^a (nt.)	3' exon ^a (nt.)	Splicing ^b k_{obs} (min ⁻¹)	Hydrolysis ^c k_{obs} (min ⁻¹)
JK43	260	624	0.50	0.05
TT1A3	48	88	0.09	0.04
TZIVS Δ 12	20	29	0.02	0.19
JK43i29	260	29	0.06	0.12
TZ Δ 12i624	20	624	0.14	0.08

^aLength of the exons in nucleotides. For TT1A3, lengths shown include both rRNA and vector sequences.

^bSplicing reactions were carried out in 100 mM ammonium sulfate, 50 mM HEPES, pH 7.5, 5 mM MgCl₂ and 100 μ M GTP, at 30°C. Rate constants were determined from linear least-squares fits to the data at initial times as described in Materials and Methods.

^cHydrolysis reactions were carried out in 50 mM CHES, pH 9.0, 200 mM NaCl and 10 mM MgCl₂, at 42°C, as described in Materials and Methods.

independent of 5' splice site recognition and addition of GTP. The rates of 3' splice site hydrolysis were measured for all three precursors, and are listed in Table I. The rate of hydrolysis measured for precursor JK43 (0.05 min⁻¹) is somewhat slower

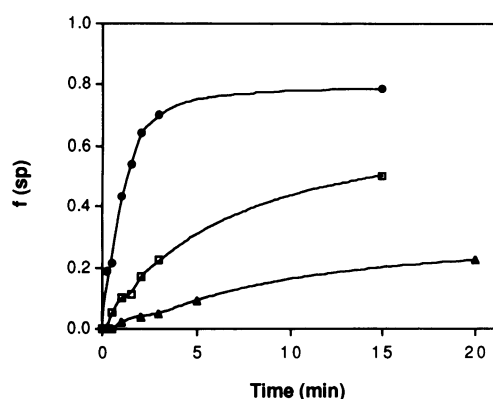


Figure 3. Fraction of Spliced Products vs. Time. Splicing reactions were carried out as described in the text. Radioactivity in each lane of the gel was quantitated, and the fraction of spliced products plotted versus time as shown. Data points are connected by an interpolated curve. ●, precursor JK43; □, TT1A3; ▲, TZIVSΔ12.

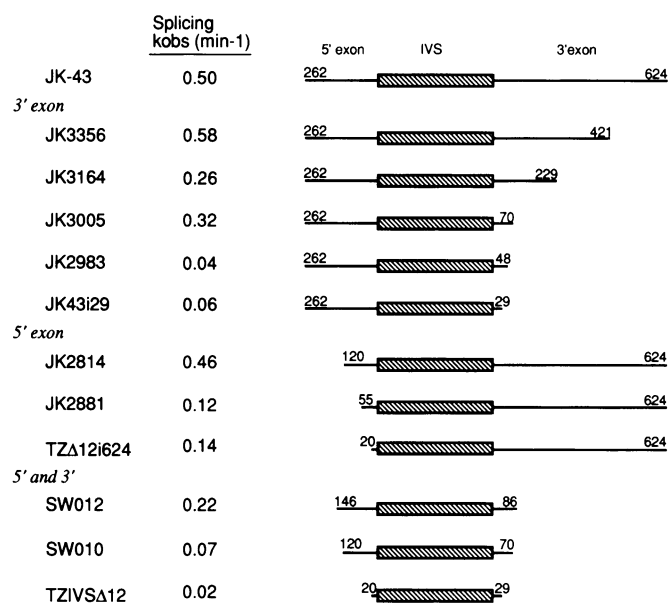


Figure 4. Splicing of Precursors with Deletions in the Exon Sequences. Precursors are diagrammed to scale, with the length of the exons shown in nucleotides. The IVS is represented by a hatched box. The observed rate constant of splicing, k_{obs} , is listed for each precursor, and was measured under standard conditions as described in Materials and Methods. Due to variations between preparations of a given precursor RNA, the uncertainty in k_{obs} is 20%, although the fit to an individual data set is typically precise ($R^2 > 0.98$).

than that of TZIVSΔ12 (0.19 min^{-1}). As can be seen in Figure 2, hydrolysis products accumulate even under normal splicing conditions for TZIVSΔ12 RNA, whereas this is not observed for precursor JK43. This agrees with my previous observation that 3' splice site hydrolysis is enhanced in precursors that preferentially form P(-1), and is perhaps related to the fact that the IGS is unpaired. Hydrolysis at the 3' splice site does not lead to formation of ligated exons. Thus not only is splicing more efficient in the longer transcript, but a non-productive side reaction is depressed.

Requirement for sequences in both exons

In order to determine whether 5' or 3' exon sequences in JK43-T₇ are responsible for its greater reactivity, precursors containing either the long 5' exon of JK43 and the short 3' exon of TZIVSΔ12, or the short 5' exon and the long 3' exon, were compared. Rates of splicing were measured as above, and are listed in Table I. As anticipated, precursor TZΔ12i624, which contains the short 5' exon and long 3' exon, splices somewhat more slowly than JK43 (0.14 min^{-1}). More surprisingly, precursor JK43i29, which contains the long 5' exon but a short 3' exon, splices poorly (0.06 min^{-1}). These results strongly suggest that sequences downstream as well as upstream of the IVS are required for maximal splicing of these transcripts.

External deletions in the exon sequences

To determine further which portions of the ribosomal exons are required for rapid splicing, deletions of either the 5' or the 3' exon were constructed. Splicing rates were measured as before, and the data are summarized in Figure 4. Again, reactivity of the pre-RNA appears to be sensitive to deletions in the 3' exon. The 3' exon can be shortened to 70 nucleotides (JK3005, 0.32 min^{-1}) with only a slight loss of reactivity. If it is truncated at 48 nucleotides (JK2983), however, the rate of splicing drops to 0.04 min^{-1} , similar to that of JK43i29 and TZIVSΔ12. The 5' exon can be reduced to 120 nucleotides in precursor JK2814 without loss of activity. Precursor JK2881, however, contains a 55 nucleotide 5' exon and splices at a rate similar to that of TZΔ12i624.

In order to construct a shorter transcript that retained most of the activity of precursor JK43, deletions were made in both exons. Initially, both exons were shortened to the same points where the individual exon deletions are still active. The resulting precursor, SW010, contains the 120 nt. 5' exon of JK2814 and the 70 nt. exon of JK3005. As shown on the bottom of Figure 4, precursor SW010 splices at a rate of 0.07 min^{-1} , slower than either JK3005 or JK2814. Moreover, 3' splice site hydrolysis was greatly enhanced (data not shown). To overcome this problem, exonuclease III was used to create a series of finer deletions in both the 3' and 5' exon sequences. Precursor SW012 was selected as giving a higher level of splicing activity than SW010 (0.22 min^{-1}), and a low rate of hydrolysis. This precursor includes 146 nucleotides of the 5' exon and 86 nucleotides of the 3' exon. SW012 is the shortest precursor of natural sequence obtained so far that preserves most of the self-splicing activity of the full length pre-rRNA.

Point mutations in the 3' exon can inhibit splicing

In addition to the deletions, several point mutations were introduced into the exons of the JK43 pre-rRNA. The splicing rates for these precursors are listed in Table II. The positions of the complementary base changes in the 5' and 3' exons are indicated in Figure 5 with open letters. Single and triple mutations in the 3' exon resulted in 10 to 50-fold lower rates of splicing (0.08 to 0.005 min^{-1}) than that of the wild type JK43 precursor (0.50 min^{-1}). These data confirm that the observed activities of these precursors depend on the specific sequence of the rRNA, and do not result from a general effect of exon length *per se*.

The original rationale for constructing these mutant precursors was to test a phylogenetically predicted long-range pairing between the 5' and 3' exons. My results do not strongly support the idea that this pairing is important for folding of the pre-RNA,

Table II. Splicing activity of precursors containing point mutations.

Mutations ^a	Splicing ^b k _{obs} (min ⁻¹)	Hydrolysis ^c k _{obs} (min ⁻¹)
G2318U	0.08	0.09
U2320G	0.02	0.03
A2322G	0.02	0.04
G2318U, U2320G, A2322G	0.005	0.04
U2118C, A2120C, C2122A	0.40	0.07
All six base changes of JK3'mis and JK5'mis	0.13	0.08

^aFor complete sequences, see inset to Figure 5.

^bObserved rates of splicing. See legend to Table I and Materials and Methods.

^cObserved rates of 3' splice site hydrolysis. See legend to Table I and Materials and Methods.

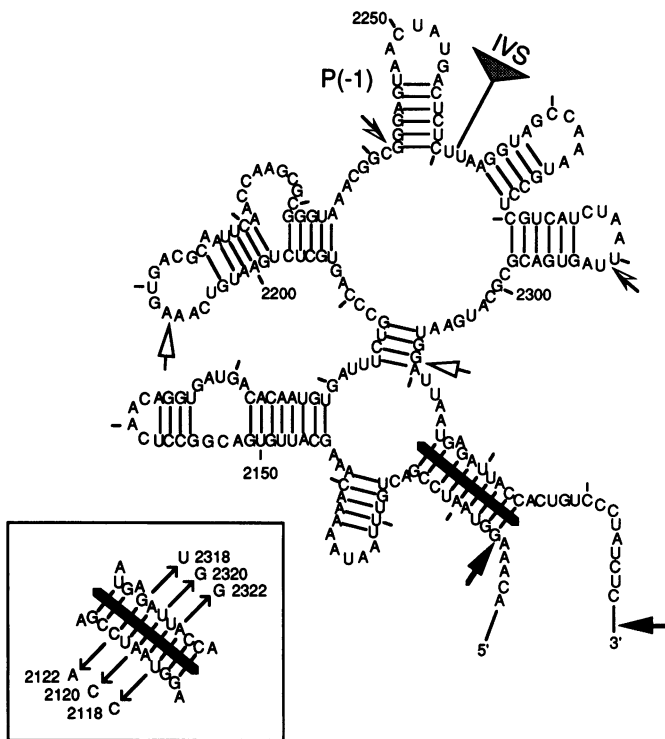


Figure 5. Sequence and secondary structure of the *Tetrahymena* 26 S rRNA in the region of the IVS. The helical stems shown match those predicted for large subunit rRNAs (23, 24), and are supported by the *Tetrahymena* sequence (25). The folding of the exon sequences in the pre-rRNA has not been experimentally determined. The position of the splice junction is marked by 'IVS', and occurs after nucleotide 2261 of the 26 S RNA (position 1925 in *E. coli*). The alternative hairpin P(-1) is indicated. Solid arrowheads mark the limits of the SW012 exons, open arrowheads denote precursors that are less reactive (JK2881 and JK2983), and the half-solid arrowheads denote the ends of precursor TZIVSΔ12. Inset: Diagram of complementary point mutations listed in Table II. The base pairing shown in the inset corresponds to the shaded helix at the bottom of the main figure.

since changes in the 5' exon (JK5'mis) had no effect on splicing activity. On the other hand, restoration of the ability to base pair in precursor JK5'3'mis does increase the observed rate of splicing over that of JK3'mis, although not to the level of the wild type RNA. The data are consistent with the results from the external deletions. If this region of the 3' exon is removed, the rate of

splicing drops significantly (JK2983, 0.04 min⁻¹). Deletion of the 5' side of this stem causes very little change in reactivity (JK2814, 0.46 min⁻¹). Although this particular long-range pairing may not be present in the protein-free pre-rRNA *in vitro*, the 3' exon sequences appear to participate in some interaction necessary for stabilizing the active form of the precursor.

DISCUSSION

The data presented here and in ref. (10) show that the self-splicing reaction of the *Tetrahymena* IVS can be strongly modulated by the nature of the exon sequences. A stable stem-loop adjacent to the 5' splice site, P(-1), has the potential for competing with formation of P1, thereby inhibiting excision of the intron. Precursors with longer exons, however, still splice efficiently, even though they contain the sequences of P(-1). I have shown that at least 146 nucleotides of the natural 5' exon sequences and 86 nucleotides of the 3' exon are required for rapid self-splicing of *Tetrahymena* pre-rRNAs *in vitro*.

The means by which the ribosomal exons contribute to excision of the IVS is not yet known. Any mechanism, however, must provide for the destabilization of P(-1) relative to P1. Formation of P(-1) is preferred in short precursors, and has been shown to result in the loss of G-addition to the 5' splice site. In principle, the presence of secondary structure in the exons could inhibit recognition of both splice sites. Thus, the enhanced reactivity of longer precursors might also be attributable to better recognition of the 3' splice site during the second step of splicing. Accumulation of 5' exon-IVS intermediate, however, is not observed during splicing of these precursors, suggesting that the first step of the reaction is still rate limiting. In preliminary experiments, the rate of intermolecular splicing to an exogenous 5' exon RNA is similar to that of intramolecular splicing for JK43, again suggesting that the 3' splice site is activated for exon ligation (23).

Clearly, sequences from both exons are required for optimal reactivity. One general observation from these data is that two different thresholds of splicing activity are reached, depending on which exon is altered. Changes in the 5' exon result in a minimum splicing rate of 0.12 ± 0.02 min⁻¹, whereas changes to the 3' exon result in a minimum rate of 0.03 ± 0.02 min⁻¹. This suggests that two (or more) means of stabilizing the active conformer may be present.

The requirement for nucleotides distant from either splice site argues that some type of long-range interaction within the RNA alters the equilibrium between P1 and P(-1). These could include another alternative pairing which destabilizes P(-1), as well as non-Watson-Crick interactions within the exons or between the exons and the IVS. Other sequences present within the longer exons may in fact be able to base pair with the 5' strand of P(-1), resulting in a higher rate of splicing (23).

The involvement of non-Watson-Crick interactions is supported by the fact that the exon sequences required for efficient splicing correspond to a highly conserved region within domain IV of the large rRNA (24, 25). The sequence of the *Tetrahymena* 26 S rRNA (26) on either side of the splice junction is shown in Figure 5, arranged according to the phylogenetically predicted secondary structure. As indicated in Figure 5, the ligated exon product of precursor SW012 contains most of this region. From the phylogenetic folding, one might expect that these sequences form a local structural unit within the mature rRNA. Whether the exons adopt a similar folding in the pre-rRNA has not been

determined yet. *In vivo*, binding of proteins to the nascent pre-rRNA could further alter its structure in the vicinity of the IVS. At a minimum, the conformation of the RNA at the splice junction must change upon removal of the IVS, since P1 is required during splicing but can no longer form in the ligated exons. An intriguing possibility is that processing of the *Tetrahymena* IVS and the associated conformational change is dependent on early steps in the assembly of the 60 S ribosomal subunit.

ACKNOWLEDGEMENTS

I wish to thank Cheryl Grosshans and Anne Ritter for synthesis of oligonucleotides, Arthur Zaug for the preparation of T₇ RNA polymerase and gift of pJK43-T₇ DNA, and Douglas Julin for critical reading of the manuscript. I also thank Tom Cech for his encouragement and generous support. This work was funded by an American Cancer Society Postdoctoral Fellowship to S.W., Howard Hughes Medical Institute (to T.R.C.), and the NIH (GM46686 to S.W.).

REFERENCES

1. Green, M. R. (1991) *Ann. Rev. Cell. Biol.* **7**, 559–599.
2. Zhuang, Y. and Weiner, A. M. (1986) *Cell* **46**, 827–835.
3. Ge, H. and Manley, J. L. (1990) *Cell* **62**, 25–34.
4. Krainer, A. R., Conway, G. C., Kozak, D. (1990) *Cell* **62**, 35–42.
5. Solnick, D. (1985) *Cell* **43**, 667–676.
6. Somasekhkar, M. B. and Mertz, J. E. (1985) *Nucleic Acids Res.* **13**, 5591–5609.
7. Reed, R. and Maniatis, T. (1986) *Cell* **46**, 681–690.
8. Clouet d'Orval, B., d'Aubenton Carafa, Y., Sirand-Pugnet, P., Gallego, M., Brody, E. and Marie, J. (1991) *Science* **252**, 1823–1828.
9. Libri, D., Piseri, A. and Fiszman, M. Y. (1991) *Science* **252**, 1842–1845.
10. Cech, T. R. (1990) *Ann. Rev. Biochem.* **59**, 543–568.
11. Been, M. D. and Cech, T. R. (1986) *Cell* **47**, 207–216.
12. Waring, R. B., Towner, P., Minter, S. J., and Davies, R. W. (1986) *Nature* **321**, 133–139.
13. Woodson, S. A. and Cech, T. R. (1991) *Biochemistry* **30**, 2042–2050.
14. Freier, S. M., Kierzek, R., Jaeger, J. A., Sugimoto, N., Caruthers, M. H., Neilson, T. and Turner, D. H. (1986) *Proc. Natl. Acad. Sci. U.S.A.* **83**, 9373–9377.
15. Bass, B. and Cech, T. R. (1986) *Cell* **47**, 207–216.
16. Davanloo, P., Rosenberg, A. H., Dunn, J. J., and Studier, F. W. (1984) *Proc. Natl. Acad. Sci. USA* **81**, 2035–2039.
17. Zaug, A. J., Been, M. D. and Cech, T. R. (1986) *Nature* **324**, 349–353.
18. Price, J. V., Kieft, G. L., Kent, J. R., Sievers, E. L. and Cech, T. R. (1985) *Nucleic Acids Res.* **13**, 1871–1889.
19. Kunkel, T. A., Roberts, J. D. and Zakour, R. A. (1987) *Methods Enzymol.* **154**, 367–382.
20. Walstrum, S. A. and Uhlenbeck, O. C. *Biochemistry* **29**, 10573–10576.
21. Zaug, A. J., Kent, J. R., and Cech, T. R. (1984) *Science* **224**, 575–578.
22. Inoue, T., Sullivan, F. X. and Cech, T. R. (1986) *J. Mol. Biol.* **189**, 143–165.
23. Woodson, S. A. and Emerick, V., unpublished.
24. Noller, H. F. (1984) *Ann. Rev. Biochem.* **53**, 119–162.
25. Clark, C. G., Tague, B. W., Ware, V. C. and Gerbi, S. A. (1984) *Nucleic Acids Res.* **12**, 6197–6220.
26. Engberg, J. and Nielsen, H. (1990) *Nucleic Acids Res.* **18**, 6915–6919.